

Article

An Efficient Algorithm for De-Interleaving Staggered PRI Signals

Wenhai Cheng^{1,2,3}, Qunying Zhang^{1,2,*}, Jiaming Dong^{1,2,3}, Haiying Wang^{1,2,3}  and Xiaojun Liu^{1,2}

¹ Aerospace Information Research Institute, Chinese Academy of Sciences, Beijing 100190, China; chengwenhai18@mails.ucas.ac.cn (W.C.); dongjiaming19@mails.ucas.ac.cn (J.D.); wanghaiying20@mails.ucas.ac.cn (H.W.); lxjdr@mail.ie.ac.cn (X.L.)

² Key Laboratory of Electromagnetic Radiation and Sensing Technology, Chinese Academy of Sciences, Beijing 100190, China

³ School of Electronic, Electrical and Communication Engineering, University of Chinese Academy of Sciences, Beijing 100190, China

* Correspondence: qyzhang@aircas.ac.cn; Tel.: +86-010-5888-7408

Abstract: Resolution and mapping bandwidth are the two most important image performance indicators that reflect satellite synthetic aperture radar (SAR) imaging reconnaissance capability. The PRI-staggered signal can simultaneously achieve high resolution in azimuth and wide swath during SAR imaging, and is an important signal form of SAR. It is important for anti-SAR reconnaissance to de-interleave the staggered PRI signal from the mixed signals. To address the problem that the existing staggered signal de-interleaving algorithms cannot accommodate PRI jitter and are computationally inefficient, this paper proposes an efficient algorithm for de-interleaving staggered PRI signals. A clustering-based square sine wave interpolation method and a threshold criterion are proposed, improving computational efficiency while suppressing interference between sub-PRI and the frame period of the staggered PRI signal. In addition, a sequence retrieval algorithm incorporating matched filter theory is proposed to improve the separation accuracy of radar pulse sequences. The simulation shows that the novel algorithm can adapt to PRI jitter and de-interleave staggered PRI signals from mixed signals with high efficiency. Compared with the existing staggered signal de-interleaving algorithm, the computational efficiency is improved by an order of magnitude.

Keywords: mixed signals; pulse de-interleaving; sequence retrieval; square sine wave interpolation; staggered PRI



Citation: Cheng, W.; Zhang, Q.; Dong, J.; Wang, H.; Liu, X. An Efficient Algorithm for De-Interleaving Staggered PRI Signals. *Appl. Sci.* **2023**, *13*, 7977. <https://doi.org/10.3390/app13137977>

Academic Editors: Yin Zhang, Deqing Mao, Yulin Huang and Yachao Li

Received: 2 June 2023

Revised: 2 July 2023

Accepted: 6 July 2023

Published: 7 July 2023



Copyright: © 2023 by the authors. Licensee MDPI, Basel, Switzerland. This article is an open access article distributed under the terms and conditions of the Creative Commons Attribution (CC BY) license (<https://creativecommons.org/licenses/by/4.0/>).

1. Introduction

Radar signal de-interleaving is one of the most critical problems of radar countermeasures systems. Its performance directly affects the effectiveness of the electronic support measures (ESM) system [1]. According to different signal parameters, the signal de-interleaving algorithm can be divided into pre-de-interleaving and main de-interleaving. The pre-de-interleaving algorithm preliminarily classifies the signal by carrier frequency (CF), pulse width (PW), pulse amplitude (PA), and angle of arrival (TOA). The main de-interleaving algorithm further processes the classification results. This paper focuses on the PRI-based main de-interleaving algorithm, which uses TOA parameters to accomplish pulse signal de-interleaving.

The pulse repetition interval (RPI) is the core parameter of pulse radar signals and the crucial characteristic used to distinguish different radar radiation sources during signal de-interleaving. With the development of radar technology, various PRI modulation approaches have been developed for different radar applications. One of the essential PRI modulation types, the staggered PRI, can both provide high azimuth resolution and a broad SAR swath [2–4] while removing the blind speed of the moving target indicator (MTI) radar system [5–7]. Several pulse sequences with the same PRI value and various

beginning phases make up the staggered PRI signal. The phase intervals are referred to as sub-PRIs, and the frame period is the same PRI value as the PRI. It is challenging to estimate the frame period of the staggered PRI signal due to its sub-PRIs interference. In addition, extracting the staggered PRI signal from mixed signals is also tricky. Moreover, the complex electromagnetic environment results in dense pulse signals, a wide PRI range, PRI jitter, and pulse missing [8]. The real-time performance of the ESM system is affected by the dense pulse signals and the wide PRI range.

With the development of modern radar electronic technology, radar signal de-interleaving technology has also been improved. Typical signal de-interleaving algorithms include histogram-based de-interleaving algorithms, PRI transform-based de-interleaving algorithms, and period estimation-based de-interleaving algorithms.

The histogram-based de-interleaving algorithm is advantageous because it is fast and straightforward [9–11]. In 2019, Ge et al. [10] proposed a pulse correlation algorithm that can de-interleave staggered PRI signals. However, it is sensitive to pulse missing. In 2021, Wang et al. [11] proposed a histogram algorithm based on the association of pulse interval and single pulse. This algorithm utilizes the association of the pulse pair interval and the single pulse to obtain the pulse interval distribution matrix (PIDM). A histogram is obtained by accumulating the row of the matrix. It can de-interleave staggered PRI signals well. However, computation efficiency and sensitivity to PRI jitter are not considered. Nelson et al. proposed the PRI transform algorithm in 1993 [12]. Nishiguchi et al. proposed a correction for the traditional PRI transform algorithm [13]. The improved algorithm handles PRI jitter and pulse loss well; however, it is computationally wasteful and unable to de-interleave staggered PRI signals. Numerous enhanced algorithms based on PRI transform have been presented due to the robustness of the improved PRI transform method [14–16]. However, they are not appropriate for de-interleaving staggered PRI signals. In 1999, Sethares et al. compared the signal's projection energy on several period subspaces to determine the signal period [17]. In 2016, an orthogonal Ramanujan period subspace was established [18]. In 2020, a correlation-matching method (CMM) was proposed based on orthogonal Ramanujan period subspace [19], which adapted to staggered PRI well but was sensitive to PRI jitter. In addition, the algorithm requires prior PRI information and is computationally inefficient. In 2021, an improved algorithm based on [19] was proposed [20]. The improved algorithm can de-interleave staggered signals and adapt to PRI jitter well, but it is still computationally inefficient.

In addition to the typical de-interleaving algorithms described above, other types of signal de-interleaving algorithms have also been proposed, including signal de-interleaving algorithms based on square sine wave interpolation [21,22], signal de-interleaving algorithms based on sequence correlation [23–25], and signal de-interleaving algorithms based on machine learning [26–29]. In 2007, Jiang et al. proposed a square sine wave interpolation algorithm [21], estimating PRI with high accuracy, speed, and anti-pulse loss. However, it is sensitive to PRI jitter and unsuitable for de-interleaving staggered signals. In recent years, signal de-interleaving algorithms based on machine learning have drawn the attention of scholars. However, such algorithms are still far from application.

The existing staggered PRI signal algorithms are computationally inefficient and cannot meet the real-time requirements of ESM systems. An improved algorithm has been proposed to solve this problem. First, an improved square sine wave interpolation algorithm has been proposed, improving computational efficiency while suppressing interference between staggered PRI signals' sub-PRIs and the frame period. A sequence retrieval algorithm incorporating matched filter theory is also proposed to improve the separation accuracy of radar pulse sequences. Finally, the staggered PRI signal is extracted, and the sub-PRIs are estimated. The simulation shows that the proposed algorithm is computationally efficient, reliable, and robust for de-interleaving staggered PRI signals from mixed signals.

The contributions of this paper are summarized as follows.

1. An efficient algorithm is proposed to de-interleave staggered PRI signals from the mixed signals. The algorithm can adjust to a broad PRI range and dense pulse signals with negligible computational costs.
2. An improved square sine wave interpolation (SSWI) function is constructed, making the algorithm adapt to staggered PRI signal and PRI jitter.
3. A threshold criterion is designed for the improved SSWI algorithm, which decreases the interference between the sub-PRIs and the frame period.
4. A sequence retrieval algorithm incorporating matched filter theory is proposed, enhancing the separation accuracy of radar pulse sequences.

This paper is organized as follows. In Section 2, the TOA model of the mixed pulse sequences is constructed. Moreover, an efficient algorithm is proposed. In Section 3, the superiority and robustness of the proposed algorithm are verified by comparative and semi-physical simulation experiments. Moreover, the computational costs are analyzed. Finally, Section 4 concludes this paper.

2. Problem Formulation and Proposed Algorithm Description

The TOA model of the mixed pulse sequences is built in this part. Additionally, an efficient algorithm for de-interleaving staggered PRI signals is provided.

2.1. The TOA Model of the Mixed Pulse Sequences

Let $t_n, n = 1, 2, \dots, N$ be the TOA of pulses, where N is the number of pulses. The TOA model of N pulses is denoted by a set T

$$T = \{t_1, t_2, \dots, t_N\} \quad (1)$$

The TOA model of the mixed pulse sequences can be expressed by the formula

$$T = \bigcup_{i=1}^K (T_i - T_{m_i}) + T_j \quad (2)$$

where K denotes the radar radiation source number, T_{m_i} indicates the missing pulses of the i -th radar, and T_j represents the set of jamming pulses.

The mixed pulse sequences in this study consider the complex PRI modulation, the pulse missing, the jamming pulses, and the noise. The TOA models of the mixed pulse sequences are shown in Figure 1.

Represent the TOA model as a discrete signal. It is as follows

$$\begin{cases} x[n] = \sum_{i=1}^K x_i[r] \\ x[n] = t_n, t_n \in T, n \in [1, N] \end{cases} \quad (3)$$

where $x_i[r]$ represents the discrete signal corresponding to the i -th radar TOA model, $x[n]$ represents the discrete signal corresponding to the TOA model of mixed pulse sequences, and T denotes the TOA set of mixed pulse sequences. The signal de-interleaving problem in this study is to obtain $x_i[r]$ according to $x[n]$.

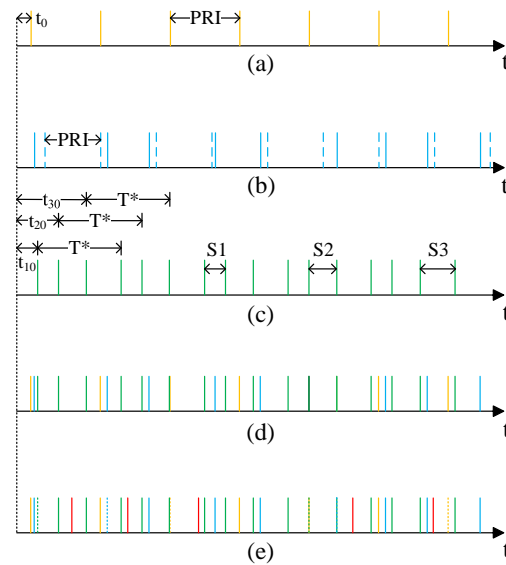


Figure 1. The TOA models of the mixed pulse sequences: (a) Fixed PRI sequence; (b) Jitter PRI sequence; (c) Staggered PRI sequence, where t_{10} , t_{20} and t_{30} represent the initial phase, T^* represents the frame period, S1, S2 and S3 represent the sub-PRI; (d) Mixed pulse sequences; (e) Mixed pulse sequences include missing pulses and jamming pulses.

2.2. The Principle and Flow of the Proposed Algorithm

For the de-interleaving of staggered PRI signals, the following issues must be resolved because of the complex electromagnetic environment.

1. The problem of suppressing the interference between the sub-PRI and the frame period.
2. The problem of extracting the staggered PRI sequence from the mixed pulse sequences.
3. The problem of computing efficiently.

An improved algorithm is proposed to solve the problems. The improved square sine wave interpolation (SSWI) algorithm is proposed to estimate the PRI value. The sequence retrieval algorithm incorporating matched filter theory is proposed to separate pulse sequences. Finally, the staggered sequences are extracted by combining the matched filter theory and the intrinsic property of staggered sequences.

For the first problem, an improved SSWI algorithm is proposed. The frame period is estimated by calculating multiple difference grade SSWI functions based on cluster. The difference grade of the improved SSWI function is increased step by step. In addition, a threshold criterion is designed for the SSWI algorithm to suppress the misidentification when the difference grade is less than the stagger number. Furthermore, the estimated PRI is the potential PRI. It needs to be verified by the sequence retrieval algorithm, further reducing the frame period misidentification probability.

For the second problem, it is challenging to extract the staggered PRI sequence from mixed sequences directly due to the complexity of the staggered PRI sequence. The improved algorithm regards the TOA model of the staggered PRI sequence as multiple pulse sequences with the PRI value as the frame period. Combining the improved SSWI and sequence retrieval algorithms, only one PRI value is estimated, and the corresponding pulse sequence is extracted in each de-interleaving round. The mixed pulse sequence is separated through multiple rounds of operations. When the sequence separation is completed, the class-matched filter algorithm is used to verify whether the pulse sequence with the same PRI comes from the same radar. These sequences are extracted as a staggered PRI sequence if they come from the same radar. A sequence retrieval algorithm incorporating matched filter theory is proposed to enhance the separation accuracy of radar pulse sequences.

For the third problem, the complex electromagnetic environment results in dense pulse signals and a wide PRI range, which seriously affect the real-time performance of the de-interleaving algorithm. An improved SSWI algorithm is proposed in this study, the computational efficiency of which is almost independent of the pulse number and the range of PRI variations, significantly improving the de-interleaving efficiency of mixed signals in complex electromagnetic environments.

The flow chart of the proposed algorithm is shown in Figure 2.

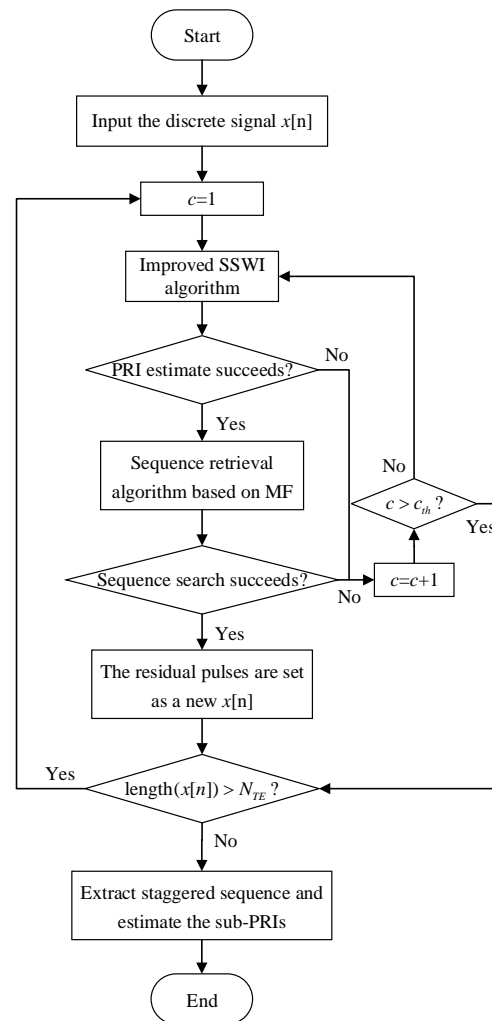


Figure 2. The flow chart of the proposed algorithm.

The flow of the proposed algorithm is as follows.

- (i) Input the discrete signal $x[n]$, initialize $c = 1$, c indicates the difference grade. Calculate the improved SSWI function, and execute the fast Fourier transform (FFT) on the interpolation result. Then, determine the estimated PRI values according to the threshold criteria, and go to Step (ii).
- (ii) Use the proposed sequence retrieval algorithm to extract the pulse sequence from the mixed discrete signal $x[n]$ by the estimated PRI. If sequence search does not succeed, $c = c + 1$. If c is greater than c_{th} , go to Step (iii); otherwise, go to Step (i). If sequence search succeeds, the residual pulses are set as a new $x[n]$. If the residual pulse number exceeds the de-interleaving threshold N_{TE} , go to Step (i); otherwise, go to Step (iii).
- (iii) Extract the staggered sequence and estimate the sub-PRIs.

2.3. Improved Square Sine Wave Interpolation Algorithm

The SSWI algorithm extracts the periodic components of the mixed pulse stream through the FFT algorithm [22]. The algorithm can suppress the influence of harmonics, interfering pulses, and missing pulses. In addition, the number of FFT points is only related to the sampling time and interpolation sampling rate. It is not affected by the pulse number and the PRI range of the input pulse stream, so the SSWI algorithm can still be computed efficiently even under dense pulses and a wide PRI range. However, the SSWI algorithm is unsuitable for staggered signals because its sub-PRI's will seriously affect the frame period estimation. The SSWI algorithm is also sensitive to PRI jitter.

An improved SSWI algorithm is proposed to solve the above problems. A clustering-based SSWI method is proposed to solve the jitter error. In addition, a threshold criterion is designed to suppress the interference of sub-PRI's on the frame period estimation. The proposed algorithm is described in detail below.

2.3.1. SSWI Function and Spectral Characteristic Analysis

The discrete signal converted by the TOA sequence is $x[n]$, $n \in [1, N]$, where N is the number of pulses. $x[i]$ ($1 \leq i \leq N$) is TOA of the i -th pulse. The difference interval of adjacent pulses is

$$\Delta t_i = x[i + 1] - x[i], i = 1, 2, \dots, N - 1 \tag{4}$$

The SSWI function is a sine wave with equal period and amplitude. The result of the SSWI function is as follows.

$$\begin{cases} s_i(t) = (\Delta t_i) \sin(\frac{2\pi}{\Delta t_i}(t - x[i])) \\ x[i] < t \leq x[i + 1], i = 1, 2, \dots, N - 1 \\ s(t) = \sum_{i=1}^{N-1} s_i(t) \end{cases} \tag{5}$$

The following formula derivation sets $x[1] = 0$. For a discrete signal with the fixed PRI, the difference interval of the discrete signal is fixed, that is, $\Delta t = \Delta t_i, i = 1, 2, \dots, N - 1$. The SSWI function for the i -th pulse interval is

$$\begin{aligned} s_i(t) &= \Delta t_i \sin(\frac{2\pi}{\Delta t_i}(t - x[i])) \\ &= \Delta t_i \sin(\frac{2\pi}{\Delta t_i}(t - (i - 1)\Delta t)) \\ &= \Delta t_i \sin(2\pi \frac{t}{\Delta t_i}), x[i] < t \leq x[N] \end{aligned} \tag{6}$$

The SSWI function of the discrete signal can be set as

$$s(t) = \Delta t \sin(2\pi \frac{t}{\Delta t}), x[1] \leq t \leq x[N] \tag{7}$$

It shows that the discrete signal with the fixed PRI is transformed into a sinusoidal signal with a single period by the SSWI, and the FFT can easily extract its period.

Jittered PRI refers to the random jitter of the PRI value around a fixed value, and the difference interval of the pulse sequence with the jittered PRI is $\Delta t_i = \Delta t'_i + \Delta \bar{t}$,

$i = 1, 2, \dots, N - 1$, where $\bar{\Delta t} = \sum_{i=1}^{N-1} \frac{\Delta t_i}{N-1}$. For a discrete signal with the jittered PRI, the SSWI function for the i -th difference interval is

$$\begin{aligned}
 s_i(t) &= (\bar{\Delta t} + \Delta t'_i) \sin\left(\frac{2\pi}{\Delta t + \Delta t'_i}(t - x[i])\right) \\
 &\approx (\bar{\Delta t} + \Delta t'_i) \sin\left(2\pi \frac{t}{\Delta t} - \frac{2\pi}{\Delta t} \sum_{j=1}^i \Delta t'_j\right), \\
 &(x[i] < t \leq x[i + 1])
 \end{aligned}
 \tag{8}$$

When the PRI jitter rate is limited to $\pm 5\%$, the SSWI function of the discrete signal with PRI jitter is an approximate sine function. Compared with the standard sine function, its spectrum will be broadened, and the spectrum value corresponding to the actual PRI value will decrease. When the PRI jitter rate exceeds $\pm 5\%$, the PRI value will not be estimated correctly from the mixed signals [21].

2.3.2. Improved SSWI Function

The previous section analyzed the spectral characteristics of the SSWI function. The PRI jitter will affect the spectrum of the SSWI function, resulting in spectrum broadening and spectral peak reduction. According to the analysis, the smaller the variance of the difference interval of the discrete signal, the more accurate the spectral estimation. A clustering-based SSWI method is proposed to solve this problem in this study. The difference interval is estimated by the clustering method and the SSWI function is generated according to the estimated difference interval.

For mixed pulse sequences, the first-grade SSWI of discrete signals may not be able to obtain the desired results due to the mutual interference of different pulse sequences. Therefore, it is necessary to calculate the multi-grade SSWI function. This paper defines the difference grade as c , where c represents the pulse interval when calculating the difference interval and initializes $c = 1$. The steps of the c -th grade improved SSWI method are as follows.

- (i) Let C_i be the i -th subclass after clustering, c_i the center value of the i -th subclass, m_i the elements number of the i -th subclass, and P the subclasses number after clustering;
- (ii) Initialization: Pulse interval sequence Δx indicates the c -th grade difference sequence of the discrete signal $x[n]$, $\Delta x = x[1 + c : N] - x[1 : N - c]$; $C_1 = \{\Delta x(1)\}$, $c_1 = \Delta x(1)$, and $j = 2$ indicates the difference interval number;
- (iii) For $p = 1 : P$, calculate the relative error between the difference interval and each cluster center

$$R_e(p) = \frac{|c_p - \Delta x(j)|}{c_p};
 \tag{9}$$

- (iv) Find the minimum of relative error vector \mathbf{R}_e . $[, p_c] = \min(\mathbf{R}_e)$, and p_c is the position corresponding to the minimum value of \mathbf{R}_e . If $R_e(p_c) < J_c$, go to Step (v); otherwise, go to Step (vi). J_c indicates the error threshold, determined by the PRI jitter upper limit;
- (v) Update subclass C_{p_c}

$$\begin{cases}
 c_{p_c} = \frac{c_{p_c} \times m_{p_c} + \Delta x(j)}{m_{p_c} + 1} \\
 m_{p_c} = m_{p_c} + 1 \\
 C_{p_c} = \{C_{p_c}, \Delta x(j)\}
 \end{cases}
 \tag{10}$$

- $j = j + 1$, update the pulse interval number, and go to Step (vii);
- (vi) Generate a new subclass and update the number of subclasses

$$\begin{cases}
 C_{P+1} = \{\Delta x(j)\}, c_{P+1} = \Delta x(j) \\
 m_{P+1} = 1, P = P + 1
 \end{cases}
 \tag{11}$$

- $j = j + 1$, update the pulse interval number, and go to Step (vii);
- (vii) If $j \leq N - c$, go to Step (iii), proceed to the next clustering; otherwise, the clustering algorithm ends, so go to Step (viii);
- (viii) Correct the difference interval sequence according to the clustering result, and generate an improved SSWI function from the corrected difference sequence.

2.3.3. A Threshold Criterion

In this subsection, a threshold criterion is designed to suppress the interference of sub-PRIs on the frame period estimation and decrease the misidentification of mixed pulse sequences. The detection threshold design process is described in detail below.

The SSWI function is shown in Formula (5). The formula shows that the continuous signal generated by the discrete signal through the SSWI can be regarded as a linear superposition of multiple continuous signals. According to the properties of the Fourier transform (FT)

If

$$\begin{cases} x(t) \overset{\mathcal{F}}{\leftrightarrow} X(j\omega) \\ y(t) \overset{\mathcal{F}}{\leftrightarrow} Y(j\omega) \end{cases} \tag{12}$$

Then

$$ax(t) + by(t) \overset{\mathcal{F}}{\leftrightarrow} aX(j\omega) + bY(j\omega) \tag{13}$$

Therefore, the FT of the SSWI function can be expressed by

$$\varphi(s(t)) = \varphi\left(\sum_{i=1}^{N-1} s_i(t)\right) = \sum_{i=1}^{N-1} \varphi(s_i(t)) \tag{14}$$

The spectral magnitude threshold of $s(t)$ is related to two factors. On the one hand, it depends on the spectral magnitude of the SSWI function $s_i(t)$; on the other hand, it depends on the number of the same difference interval.

Firstly, compute the FT of $s_i(t)$. Let $\omega_0 = \frac{2\pi}{\Delta t_i}$, and compute the FT of $s_i(t)$

$$\begin{aligned} \varphi(s_i(t)) &= \int_{x[i]}^{x[i]+\Delta t_i} \Delta t_i \sin(\omega_0 t) e^{-j\omega t} dt \\ &= \Delta t_i \frac{e^{-j(\omega_0+\omega)x[i]} - e^{-j(\omega_0+\omega)(x[i]+\Delta t_i)}}{2(\omega_0 + \omega)} \\ &\quad + \Delta t_i \frac{e^{-j(\omega_0-\omega)x[i]} - e^{-j(\omega_0-\omega)(x[i]+\Delta t_i)}}{2(\omega_0 - \omega)} \end{aligned} \tag{15}$$

The spectral amplitude is related to the number of FT points, and the algorithm calculates the number of FT points according to $s(t)$, not $s_i(t)$. Let the interpolation sample rate be F_s , and the amplitude of the one-sided spectrum of $s_i(t)$ is

$$\begin{aligned} |\varphi(s_i(t))| &= \left| \lim_{\omega \rightarrow \omega_0} \frac{e^{-j(\omega_0-\omega)x[i]} - e^{-j(\omega_0-\omega)(x[i]+\Delta t_i)}}{2(\omega_0 - \omega)} \right| \\ &\quad \cdot 2\Delta t_i \frac{F_s \cdot \Delta t_i}{F_s \cdot x[N]} \\ &= \Delta t_i^2 / x[N] \end{aligned} \tag{16}$$

The number of the same difference interval is the next concern. When the number of pulses from multiple radiation sources in the observation time is large enough, the difference interval value between adjacent pulses can be set as a random event; that is, the TOA of the pulse is set as the Poisson point. Suppose the observation time is t_N , the pulse

number is N , the difference interval is Δt_i , and the probability of k random points in the difference interval Δt_i is

$$p_k(\Delta t_i) = \frac{(\lambda \Delta t_i)^k}{k!} e^{-\lambda \Delta t_i}, k = 0, 1, 2, \dots \tag{17}$$

where $\lambda = N/t_N$ indicates the average number of events per unit time.

The probability that the difference interval between adjacent pulses is Δt_i can be derived from the previous expression for $k = 0$

$$p_0(\Delta t_i) = e^{-\lambda \Delta t_i} \tag{18}$$

As the histogram is the estimate of the probability distribution function of a random event, the histogram of higher-grade differences will also be in exponential form. The detection threshold of the difference interval Δt_i can be expressed as

$$N_\tau = \alpha(N - c)e^{-\lambda \Delta t_i} \tag{19}$$

where α is a tunable parameter, depending on the supposed maximum percentage of missed pulses.

In summary, the detection threshold of the improved SSWI algorithm is

$$\begin{aligned} A_{SW}(\Delta t_i) &= |\varphi(s_i(t))| \cdot N_\tau \\ &= \alpha \Delta t_i^2 (N - c) e^{-\lambda \Delta t_i} / x[N] \end{aligned} \tag{20}$$

The threshold criterion is stated as follows. If only one spectrum value exceeds the detection threshold, the period corresponding to the spectrum value is the estimated PRI value; if multiple spectrum values exceed the detection threshold, the period corresponding to the largest spectrum value is selected as the estimated PRI value.

2.3.4. The Flow of the Improved SSWI Algorithm

The flow of the improved SSWI algorithm is given in Algorithm 1.

Algorithm 1: The flow of the improved SSWI algorithm

Input:

- (i) Discrete signal $x[n]$;
- (ii) Difference grade c .

Improved SSWI and FFT:

- (i) Calculate the c -th grade difference sequence;
- (ii) Estimate the difference interval by clustering method and correct the difference interval;
- (iii) **For** 1 to $N - c$

Generate the SSWI function according to the corrected difference interval;

End

- (iv) Compute the FFT of the improved SSWI function.

Threshold Criterion:

- (i) Calculate the detection threshold, and compare the spectral value with threshold A_{SW} . The period values corresponding to the spectral values exceeding the detection threshold generate a set Q ;
- (ii) Select the element corresponding to the largest spectral value q in the set Q as the estimated period.

Output:

The estimated PRI is q .

2.4. Sequence Retrieval Algorithm Based on Matched Filter

Pulse sequence separation is challenging for mixed signals. The cumulative error caused by PRI jitter will lead to pulse separation error. Moreover, the interference between pulse sequences will be serious for multiple pulse sequences arriving simultaneously. A sequence retrieval algorithm is proposed in [20], which solves the cumulative error by the cumulative average method and suppresses the interference between multiple pulse sequences by the clustering method. However, the separation is inaccurate when multiple pulse sequences exist simultaneously. Based on the sequence retrieval algorithm proposed in [20], a class-matched filter algorithm is proposed to solve the interference between multiple pulse sequences in this study, enhancing the radar pulse stream’s separation accuracy significantly.

The main reason for the mutual interference of multiple pulse sequences is that multiple pulses may meet the search conditions in one search operation. If the correct pulse was not selected for the separation, the periodicity of the remaining pulse sequence would be destroyed. The class-matched filter algorithm is proposed to suppress the mutual interference in this study. By introducing sampling information of the pulse signal, multiple pulses that satisfy the search conditions are filtered.

The class-matched filter algorithm is described as follows. The multiple pulses that satisfy the search conditions can be set as

$$X(m) = [x_1(m), x_2(m), \dots, x_n(m)] \tag{21}$$

where $x_i(m) (i = 1, 2, \dots, n)$ indicates the sampled signal of the i -th pulse that satisfies the search condition. Define $N_i = \text{length}(x_i(m)), i = 1, 2, \dots, n$. The sampled signal of the reference pulse is set to $x_0(m)$, and define class-matched filter operations

$$R = x_0(m) \otimes X(m) = \begin{pmatrix} x_0(m) * x_1(N_1 - m) \\ x_0(m) * x_2(N_2 - m) \\ \vdots \\ x_0(m) * x_n(N_n - m) \end{pmatrix} = \begin{pmatrix} r_1 \\ r_2 \\ \vdots \\ r_n \end{pmatrix} \tag{22}$$

The operation $x_0(m) \otimes X(m)$ represents the correlation operation of $x_0(m)$ and each component of $X(m)$, respectively. According to the matched filter theory, the correlation operation and the matched filter are equivalent [30]. Assuming that $x_0(m)$ and $x_i(m)$ are pulses emitted by the same radiation source, there will be a peak in r_i ; otherwise, there will be no. The peak detection threshold is determined experimentally.

Assuming the discrete signal is x , the estimated PRI is q , the steps of the sequence retrieval algorithm based on matched filter theory are as follows:

- (i) Initialization: $i = 1, k_c = 1, n_c = 1$, reference pulse $t_{ref} = x[i]; k_{min}, k_{max}$, where k_{min}, k_{max} and k_c , and determine the search scope, determined by the PRI jitter upper limit; n_c is for counting;
- (ii) According to reference pulse t_{ref} and PRI value q , calculate the search scope:

$$\begin{cases} T_{max} = t_{ref} + q * k_{max} * k_c \\ T_{min} = t_{ref} + q * k_{min} * k_c \end{cases} \tag{23}$$

If $T_{max} > \max(x) * k_{max}$, this round is complete, so go to Step (vi); else, go to Step (iii).

- (iii) Search for the next pulse that meets the condition:

$$p_s = \text{find}((x \geq T_{min}) \& (x \leq T_{max})) \tag{24}$$

where $find(\bullet)$ is a function used to search for the element number that satisfies the condition, and p_s indicates the position of elements that meets the condition. If $length(p_s) = 0$, it indicates that no pulses meet the search condition; $k_c = k_c + 1$, so go to Step (ii); if $length(p_s) = 1$, it indicates that only one pulse meets the search condition, and $x[n_e] = x[p_s]$, so go to Step (v); if $length(p_s) > 1$, it indicates that multiple pulses meet the search condition, so go to Step (iv);

- (iv) Screen the next pulse by the class-matched filter operation. According to Formula (22), $x_0(m)$ is the sampling signal of the reference pulse t_{ref} , $X(m)$ is the sampling signal of the pulse set $x[p_s]$, $x[n_e]$ is determined by the class-matched filter operation; go to Step (v);
- (v) Update the PRI value based on the searched next pulse:

$$q = \frac{n_c * q + \frac{x[n_e] - t_{ref}}{k_c}}{n_c + 1} \tag{25}$$

where $x[n_e]$ indicates the next pulse found. Update reference pulse, $t_{ref} = x[n_e]$; update number of pulses, $n_c = n_c + 1$; initialization pulse interval, $k_c = 1$; go to Step (ii); continue searching for the next pulse of the new reference pulse;

- (vi) If n_c exceeds N_{TH} , end the pulse sequence search; else, $i = i + 1$. If i is greater than $(length(x[n]) - N_{TH})$, end the pulse sequence search; otherwise, update reference pulse, $t_{ref} = x[i]$; initialization $n_c = 1, k_c = 1$; go to Step (ii).

The flow of the sequence retrieval algorithm incorporating matched filter theory is shown in Figure 3.

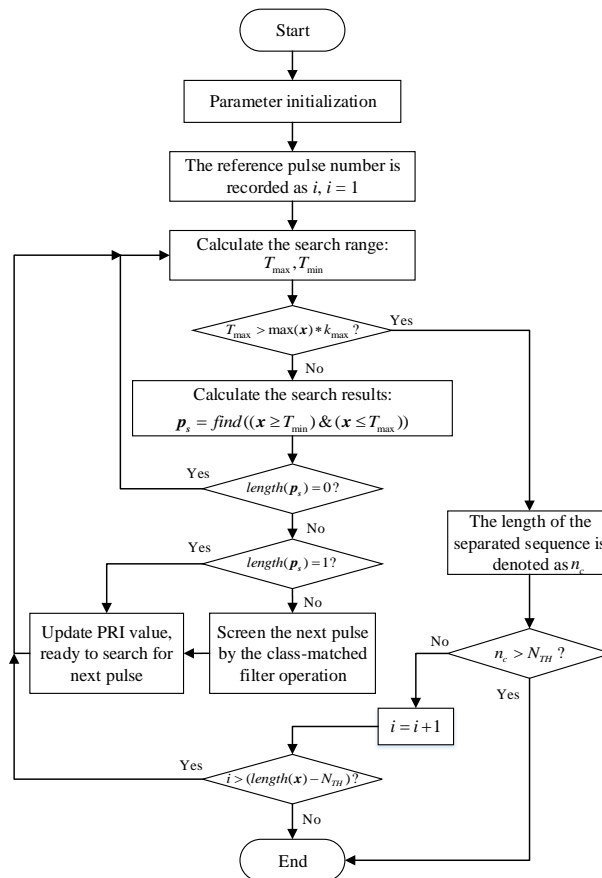


Figure 3. The flow chart of the sequence retrieval algorithm based on matched filter theory.

2.5. Extract the Staggered PRI Sequence and Estimate the Sub-PRI

The class-matched filter algorithm is used to determine whether the pulse sequence with the same PRI originates from the same radar after the sequence separation. The pulse sequences with the same PRI are recovered as a staggered sequence if they originate from the same radar. The difference histogram approach is used to estimate the sub-PRI. Considering the effect of PRI jitter, a clustering histogram method is proposed. The clustering method is the same as Section 2.3.2, "Improved Square Sine Wave Interpolation Function".

3. Simulation and Analysis

This section verifies the performance of the proposed algorithm. In Section 3.1, the de-interleaving process is introduced in detail, and each step's result is given. In Section 3.2, the simulation comparison experiments evaluate and analyze the algorithm performance. In Section 3.3, the analysis of the computational cost is given. Finally, a semi-physical simulation experiment is executed to validate the proposed algorithm.

3.1. Simulation Experiments

Assuming a mixed pulse stream is interleaved by four TOA sequences arriving simultaneously. The parameter setting of the mixed pulse stream is referred to [11,19,31], which are the latest results for staggered signal de-interleaving. Pulse Sequence 1 is a staggered PRI signal, and the staggering number is five; Pulse Sequence 2 is a jittered signal; the remaining two signals are fixed PRI signals. The parameters of the TOA model are shown in Table 1. The jamming pulses are not shown in the table. The de-interleaving process of the proposed algorithm is introduced as follows:

In the initial de-interleaving round, no PRI is detected in the first two-grade SSWI function. A PRI is detected in the third-grade SSWI function, but the corresponding pulse sequence is not searched. The FFT of the fourth-grade SSWI function is shown in Figure 4a, the estimated PRI value is 165.9 μ s. The second through eighth rounds of de-interleaving are similar to the first round. The results are shown in Figure 4b–h.

After the eighth round of de-interleaving, the number of residual pulses is seldom. All pulse sequences have been separated. Then, extract the staggered pulse sequence and estimate the sub-PRI. The frame period of the staggered pulse sequence is $(165.9 * 2 + 165.5 * 2 + 165.1) / 5 = 165.6 \mu$ s, and the sub-PRI are 11 μ s, 20 μ s, 32.8 μ s, 45 μ s, and 56.5 μ s, respectively. The simulation of the sub-PRI estimation is shown in Figure 5.

Define m_{error} as follows:

$$m_{error} = \frac{1}{n} \sum_{i=1}^n \frac{|P_{e_i} - P_i|}{P_i} \quad (26)$$

where P_{e_i} is the estimated PRI value, P_i is the setting PRI value, and n is the number of radar radiation sources.

The m_{error} of the simulation is as follows:

$$\begin{aligned} m_{error} &= \frac{1}{4} \left(\frac{|165.6 - 166|}{166} + \frac{|442.8 - 441|}{441} \right. \\ &\quad \left. + \frac{|780.2 - 780|}{780} + \frac{|1150 - 1151|}{1151} \right) \\ &= 0.21\% \end{aligned} \quad (27)$$

The simulation showed that the proposed algorithm can de-interleave staggered PRI signals and estimate sub-PRI of the staggered signal with high estimation accuracy.

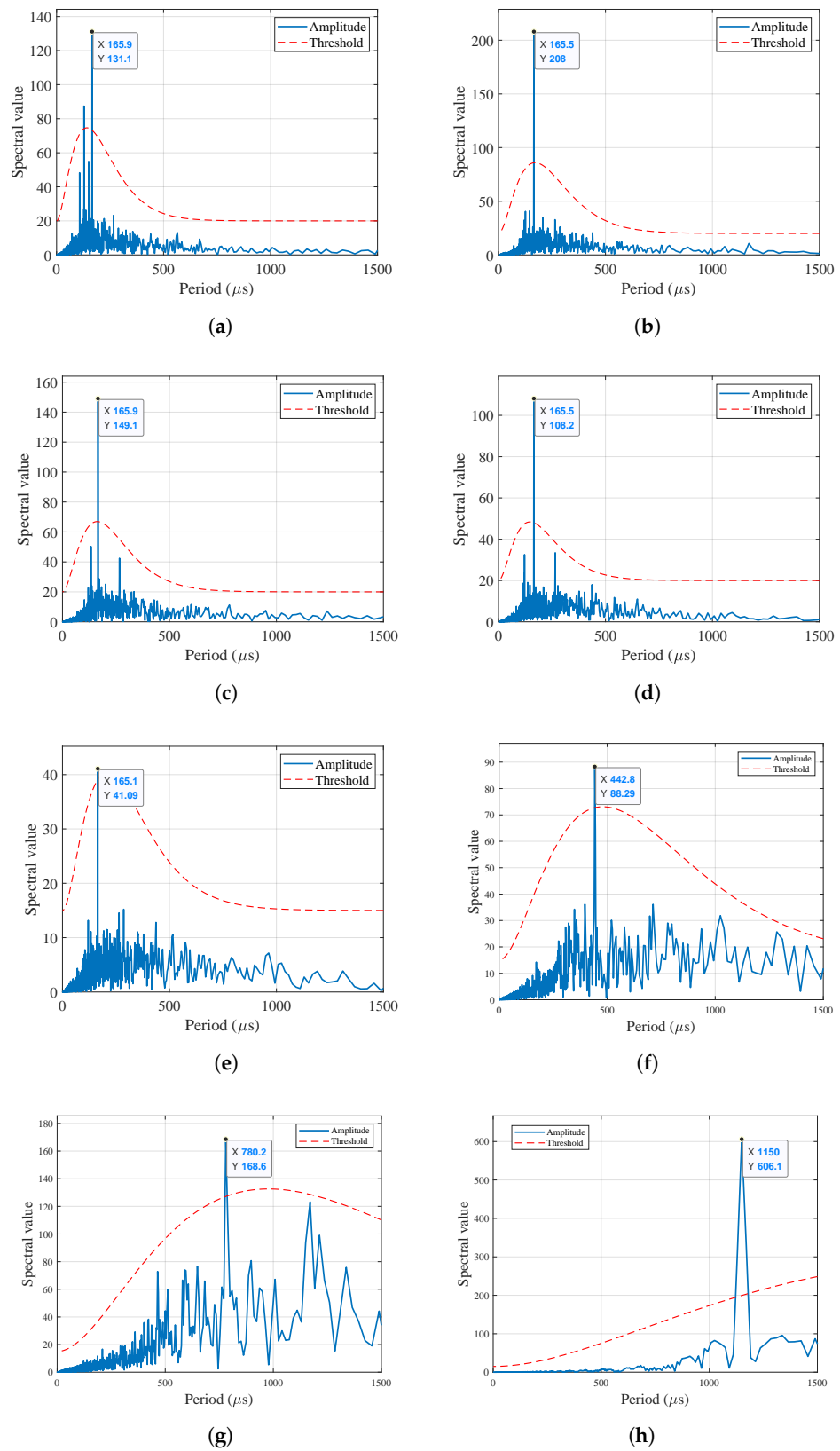


Figure 4. The de-interleaving results: (a) The first round; (b) The second round; (c) The third round; (d) The fourth round; (e) The fifth round; (f) The sixth round; (g) The seventh round; (h) The eighth round.

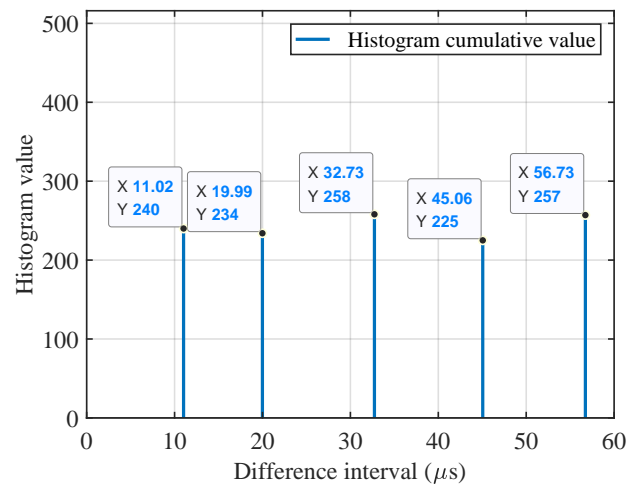


Figure 5. Sub-PRI estimation result of staggered PRI signal.

Table 1. Parameters of Mixed Pulse Stream 1.

	Pulse Sequence 1	Pulse Sequence 2	Pulse Sequence 3	Pulse Sequence 4
PRI modulation type	Staggered	Jittered	Fixed	Fixed
Frame period (μs)	166	-	-	-
Sub-PRI (μs)	11, 20, 33, 45, 57	-	-	-
PRI value (μs)	-	441	780	1151
Noise error (μs)	± 0.5	± 0.5	± 0.5	± 0.5
Jitter bound	0	$\pm 10\%$	0	0
Missing rate	10%	15%	20%	20%
Observation time (μs)	50,000	50,000	50,000	50,000

3.2. Comparative Experiments

This section analyzes the algorithm's performance under different PRI jitter, missing pulses, and radiation source numbers. The signal de-interleaving algorithm is based on sequence correlation [11], and the signal de-interleaving algorithm is based on CMM [19] as the latest results were used for comparison. The parameters used for the simulation are as follows: the number of pulses of a single pulse sequence is 100; the stagger number is set to 3; the PRI range is [100 μs , 500 μs]. Measure five times consecutively, and the de-interleaving result with the lowest number of correctly extracted radiation sources among the five tests was selected as the final result. The simulations are shown in Tables 2 and 3. As shown in Tables 2 and 3, the following hold.

- (i) The algorithm proposed in this research can correctly de-interleave five radiation source signals arriving simultaneously when the PRI jitter rate is $\pm 12\%$ and the pulse missing rate is 5%. The algorithm proposed in this research can correctly de-interleave four radiation source signals arriving simultaneously when the PRI jitter rate is $\pm 3\%$ and the pulse missing rate is 15%. The proposed approach for signal de-interleaving is highly suited to PRI jitter and pulse missing.
- (ii) The signal de-interleaving algorithm based on sequence correlation is sensitive to PRI jitter. In addition, the performance of the sequence correlation algorithm for fixed PRI signals de-interleaving decreases as the pulse missing rate increases. When the pulse missing rate increases, the peak of the line histogram corresponding to the true PRI decreases, and the peak of the line histogram corresponding to the PRI harmonics increases, so the harmonic components of the true PRI are detected, resulting in de-interleaving errors. Due to the characteristics of staggered signals, pulse loss has less impact on the de-interleaving of the staggered PRI signal. Even if the pulse loss is severe, the line histogram peak corresponding to the frame periods is still high.

- (iii) The CMM-based signal de-interleaving algorithm is sensitive to PRI jitter. The effectiveness of the CMM-based signal de-interleaving algorithm declines as the pulse missing rate and number of radar radiation sources rise. When the pulse missing rate is considerable, the sequence retrieval is greatly affected by the interference of different pulse sequences, resulting in wrong pulse separation and consequently to de-interleaving errors.
- (iv) As the pulse missing rate and the number of radiation sources increase, the performance of the proposed algorithm is better than the algorithms in [11,19]. The proposed algorithm adopts two measures to improve de-interleaving success rate. The probability of misidentification is reduced by combining the improved SSWI algorithm and sequence retrieval algorithm. Moreover, based on the matched filter theory, a sequence retrieval algorithm is proposed, enhancing the pulse sequence's separation accuracy.

Table 2. Comparison results of three algorithms under different PRI jitter rates.

PRI Jitter Rate	Missing Rate	Input Radiation Source Conditions	De-Interleaving Results		
			Sequence Correlation	CMM	Ours
±4%	5%	1 staggered PRI	1/1	1/1	1/1
±4%	5%	1 staggered PRI and 1 fixed PRI	1/2	1/2	2/2
±4%	5%	1 staggered PRI and 2 fixed PRI	1/3	1/3	3/3
±4%	5%	2 staggered PRI and 2 fixed PRI	2/4	2/4	4/4
±4%	5%	2 staggered PRI and 3 fixed PRI	2/5	2/5	5/5
±8%	5%	1 staggered PRI	1/1	1/1	1/1
±8%	5%	1 staggered PRI and 1 fixed PRI	1/2	1/2	2/2
±8%	5%	1 staggered PRI and 2 fixed PRI	1/3	1/3	3/3
±8%	5%	2 staggered PRI and 2 fixed PRI	2/4	2/4	4/4
±8%	5%	2 staggered PRI and 3 fixed PRI	2/5	2/5	5/5
±12%	5%	1 staggered PRI	1/1	1/1	1/1
±12%	5%	1 staggered PRI and 1 fixed PRI	1/2	1/2	2/2
±12%	5%	1 staggered PRI and 2 fixed PRI	1/3	1/3	3/3
±12%	5%	2 staggered PRI and 2 fixed PRI	2/4	2/4	4/4
±12%	5%	2 staggered PRI and 3 fixed PRI	2/5	2/5	5/5

Table 3. Comparison results of three algorithms under different pulse missing rate.

Missing Rate	Input Radiation Source Conditions	De-Interleaving Results		
		Sequence Correlation	CMM	Ours
5%	1 staggered PRI	1/1	1/1	1/1
5%	1 staggered PRI and 1 fixed PRI	2/2	2/2	2/2
5%	1 staggered PRI and 2 fixed PRI	3/3	3/3	3/3
5%	2 staggered PRI and 2 fixed PRI	4/4	4/4	4/4
5%	2 staggered PRI and 3 fixed PRI	5/5	5/5	5/5
10%	1 staggered PRI	1/1	1/1	1/1
10%	1 staggered PRI and 1 fixed PRI	2/2	2/2	2/2
10%	1 staggered PRI and 2 fixed PRI	3/3	3/3	3/3
10%	2 staggered PRI and 2 fixed PRI	3/4	4/4	4/4
10%	2 staggered PRI and 3 fixed PRI	4/5	4/5	5/5
15%	1 staggered PRI	1/1	1/1	1/1
15%	1 staggered PRI and 1 fixed PRI	2/2	2/2	2/2
15%	1 staggered PRI and 2 fixed PRI	3/3	3/3	3/3
15%	2 staggered PRI and 2 fixed PRI	2/4	3/4	4/4
15%	2 staggered PRI and 3 fixed PRI	3/5	3/5	4/5

3.3. Computational Costs

This section analyzes the computational complexity of the three algorithms (Refs. [11,19] and ours) and compares the simulation time of the three algorithms under different radiation source conditions.

Suppose the prior PRI range is $[PRI_{min}, PRI_{max}]$, where PRI_{min} indicates the minimum PRI value; PRI_{max} indicates the maximum PRI value; K is the number of PRI bins, determined by estimation accuracy and PRI range; N is the number of pulses; H indicates the stagger number [11]; L_1 indicates the length of the converted period sequence, determined by estimation accuracy and observation time; $\phi(q)$ is the Euler function; β is determined by PRI range and observation time [19]; L_2 indicates the length of the SSWI function, determined by estimation accuracy and observation time; and M is the number of points used for matched filter. The computational complexity of the three de-interleaving algorithms is shown in Table 4.

A comparison of the execution time among the three methods is shown in Table 5, MATLAB 2018b is utilized for computation time statistics.

The simulation shows that the computational efficiency of the algorithm proposed in this study is much higher than the algorithms in Refs. [11,19] for multiple radiation source scenes. Table 4 shows that the computational efficiency of the proposed algorithm in this study mostly depends on the observation time and the number of matched filter points. The computational efficiency is little affected by the number of radiation sources and also unaffected by the PRI range. Therefore, the proposed algorithm has obvious advantages for the multiple radiation sources scene and wide PRI range in computational efficiency.

Table 4. The computational complexity of the three de-interleaving algorithms.

Sequence Correlation	Part1	$O(N^2)$
	Part2	$O(KN)$
	Part3	$O(H^2 \log H)$
	Total	$O(N^2 + KN)$
CMM	Part1	$O(\beta N^2) + O(L_1 \sum_{q=PRI_{min}}^{PRI_{max}} \phi(q))$
	Part2	$O(N)$
	Part3	$O(N)$
	Total	$O((\beta N^2) + O(L_1 \sum_{q=PRI_{min}}^{PRI_{max}} \phi(q)))$
Ours	Part1	$O(L_2 \log(L_2))$
	Part2	$O(N + M \log(M))$
	Part3	$O(N)$
	Total	$O(L_2 \log(L_2)) + O(N + M \log(M))$

Table 5. Execution time of the three de-interleaving algorithms.

PRI Range	Radiation Sources	Sequence Correlation	CMM	Ours
100–300	2	2.21 s	4.15 s	0.91 s
100–300	4	6.73 s	7.22 s	1.13 s
100–300	6	10.25 s	13.57 s	1.37 s
100–600	2	3.62 s	8.62 s	0.92 s
100–600	4	10.51 s	12.51 s	1.11 s
100–600	6	16.33 s	19.25 s	1.35 s
100–1000	2	5.51 s	14.22 s	0.95 s
100–1000	4	16.62 s	17.52 s	1.21 s
100–1000	6	24.33 s	24.76 s	1.39 s

3.4. Semi-Physical Simulation Experiments

This section validates the proposed algorithm through a semi-physical simulation experiment. The semi-physical simulation process is shown in Figure 6. First, the radar signal simulator simulates multiple radar signals arriving simultaneously. Then, the reconnais-

since jammer measures the simulated radar signals' parameters. Finally, the measured TOA sequence is uploaded to the computer to verify the proposed de-interleaving algorithm.

The parameter settings of the radar signal simulator are shown in Table 6, and the results are shown in Figure 7. The semi-physical simulation shows that the proposed algorithm can de-interleave staggered PRI signals and estimate the sub-PRI of staggered signals.

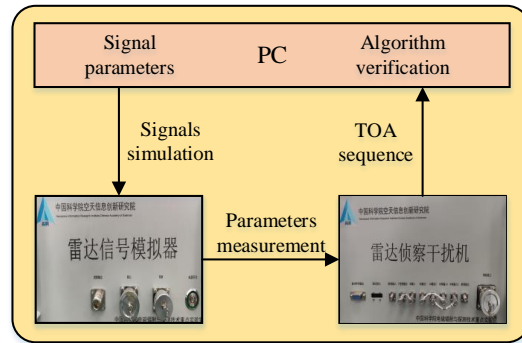


Figure 6. The semi-physical simulation process.

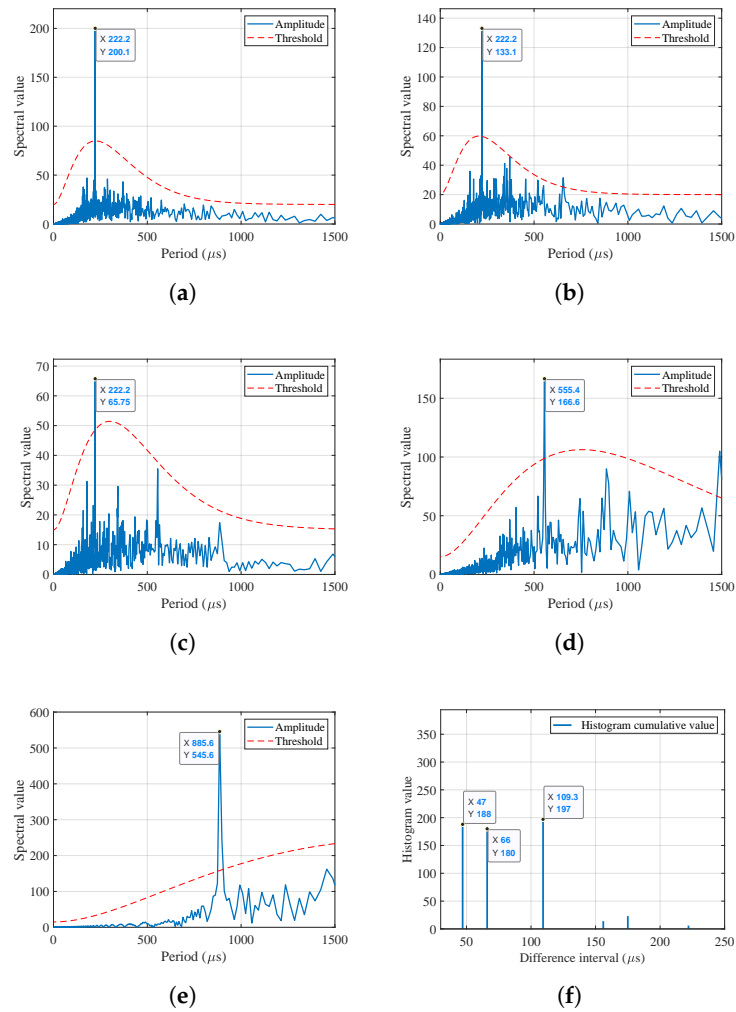


Figure 7. The semi-physical simulation of the proposed algorithm: (a) The first round; (b) The second round; (c) The third round; (d) The fourth round; (e) The fifth round; (f) Sub-PRI estimation result.

Table 6. Parameters of Mixed Pulse Stream 2.

	Sequence 1	Sequence 2	Sequence 3
PRI modulation type	Staggered	Jittered	Fixed
Frame period (μs)	222	-	-
Sub-PRIs (μs)	47, 66, 109	-	-
PRI value (μs)	-	555	887
Jitter bound	0	$\pm 10\%$	0

4. Conclusions

This paper proposes an efficient algorithm to de-interleave staggered PRI signals. Firstly, an improved SSWI method is proposed to enhance the adaptability to PRI jitter. In addition, a threshold criterion is designed for the improved SSWI algorithm, which decreases the interference between the sub-PRIs and the frame period. A sequence retrieval algorithm incorporating matched filter theory is proposed, enhancing the separation accuracy of radar pulse sequences. Finally, the staggered sequences are extracted by combining the matched filter theory and intrinsic properties of staggered sequences. Simulation experiments have validated the proposed algorithm's superiority for de-interleaving staggered PRI signals from mixed signals.

However, the algorithm proposed in this paper also has limitations. The proposed algorithm uses the difference information of the TOA sequence to estimate the PRI, and the difference grade gradually increases. When the mixed TOA sequence is complex enough, due to the mutual interference of different pulse sequences, misidentification may occur. The next research work is to de-interleave staggered PRI signals from dense and complex radar signals with high efficiency.

Author Contributions: Conceptualization, W.C. and Q.Z.; methodology, W.C. and J.D.; validation, J.D., H.W. and W.C.; software, H.W. and W.C.; writing—original draft preparation, W.C.; writing—review and editing, Q.Z.; visualization, W.C.; supervision, X.L.; project administration, Q.Z. and X.L.; funding acquisition, Q.Z. All authors have read and agreed to the published version of the manuscript.

Funding: This research received no external funding.

Institutional Review Board Statement: Not applicable.

Informed Consent Statement: Not applicable.

Data Availability Statement: Not applicable.

Acknowledgments: The authors would like to thank the editors and reviewers for their efforts to help the publication of this work.

Conflicts of Interest: The authors declare no conflict of interest.

References

- Butt, F.A.; Jalil, M. An overview of electronic warfare in radar systems. In Proceedings of the 2013 The International Conference on Technological Advances in Electrical, Electronics and Computer Engineering (TAECE), Konya, Turkey, 9–11 May 2013; pp. 213–217. [\[CrossRef\]](#)
- Villano, M.; Krieger, G.; Jäger, M.; Moreira, A. Staggered SAR: Performance Analysis and Experiments With Real Data. *IEEE Trans. Geosci. Remote Sens.* **2017**, *55*, 6617–6638. [\[CrossRef\]](#)
- de Almeida, F.Q.; Rommel, T.; Younis, M.; Krieger, G.; Moreira, A. Multichannel Staggered SAR: System Concepts With Reflector and Planar Antennas. *IEEE Trans. Aerosp. Electron. Syst.* **2019**, *55*, 877–902. [\[CrossRef\]](#)
- Aldharrab, A.; Davies, M.E. Staggered Coprime Pulse Repetition Frequencies Synthetic Aperture Radar (SCopSAR). *IEEE Trans. Geosci. Remote Sens.* **2022**, *60*, 5208711. [\[CrossRef\]](#)
- McAulay, R.J. The Effect of Staggered PRF's on MTI Signal Detection. *IEEE Trans. Aerosp. Electron. Syst.* **1973**, *AES-9*, 615–618. [\[CrossRef\]](#)
- Houts, R.C.; Crabtree, S.B. The Effect of MTI Filter and Number of Unique Staggers on First-Null Depth and Clutter Attenuation. *IEEE Trans. Aerosp. Electron. Syst.* **1979**, *AES-15*, 163–168. [\[CrossRef\]](#)
- Ispir, M.; Candan, C. On the design of staggered moving target indicator filters. *IET Radar Sonar Navig.* **2016**, *10*, 205–215. [\[CrossRef\]](#)

8. He, C.; Zhu, X.; Zhang, G. Interception Analysis of Radar Countermeasure Reconnaissance System. In Proceedings of the 2013 5th International Conference on Intelligent Human-Machine Systems and Cybernetics, Hangzhou, China, 26–27 August 2013; Volume 1, pp. 532–535. [[CrossRef](#)]
9. Liu, Y.; Zhang, Q. Improved method for deinterleaving radar signals and estimating PRI values. *IET Radar Sonar Navig.* **2018**, *12*, 506–514. [[CrossRef](#)]
10. Ge, Z.; Sun, X.; Ren, W.; Chen, W.; Xu, G. Improved algorithm of radar pulse repetition interval deinterleaving based on pulse correlation. *IEEE Access* **2019**, *7*, 30126–30134. [[CrossRef](#)]
11. Wang, J.; Huang, Y. Stagger pulse repetition interval pulse train de-interleaving algorithm based on sequence association. *J. Electron. Inf. Technol.* **2021**, *43*, 1145–1153. [[CrossRef](#)]
12. Nelson, D. Special purpose correlation functions for improved signal detection and parameter estimation. In Proceedings of the 1993 IEEE International Conference on Acoustics, Speech, and Signal Processing, Minneapolis, MN, USA, 27–30 April 1993; Volume 4, pp. 73–76. [[CrossRef](#)]
13. Nishiguchi, K.; Kobayashi, M. Improved algorithm for estimating pulse repetition intervals. *IEEE Trans. Aerosp. Electron. Syst.* **2000**, *36*, 407–421. [[CrossRef](#)]
14. Cheng, B.; Han, J.. A new method of radar signal sorting based on the PRI transform and wavelet transform. In Proceedings of the 11th International Conference on Wireless Communications, Networking and Mobile Computing (WiCOM 2015), Shanghai, China, 21–23 September 2015; pp. 1–4. [[CrossRef](#)]
15. Mahdavi, A.; Pezeshk, A.M. A fast enhanced algorithm of PRI transform. In Proceedings of the 2011 Sixth International Symposium on Parallel Computing in Electrical Engineering, Luton, UK, 3–7 April 2011; IEEE: Piscataway, NJ, USA, 2011; pp. 179–184. [[CrossRef](#)]
16. Xi, Y.; Wu, X.; Wu, Y.; Deng, L. A Fast and Real-time PRI Transform Algorithm for Deinterleaving Large PRI Jitter Signals. In Proceedings of the 2018 37th Chinese Control Conference (CCC), Wuhan, China, 25–27 July 2018; IEEE: Piscataway, NJ, USA, 2018; pp. 4465–4469. [[CrossRef](#)]
17. Sethares, W.A.; Staley, T.W. Periodicity transforms. *IEEE Trans. Signal Process.* **1999**, *47*, 2953–2964. [[CrossRef](#)]
18. Pei, S.C.; Chang, K.W. Closed-Form Orthogonal Ramanujan Integer Basis. *IEEE Signal Process. Lett.* **2016**, *24*, 116–120. [[CrossRef](#)]
19. Tao, J.W.; Yang, C.Z.; Xu, C.W. Estimation of PRI Stagger in Case of Missing Observations. *IEEE Trans. Geosci. Remote. Sens.* **2020**, *58*, 7982–8001. [[CrossRef](#)]
20. Cheng, W.; Zhang, Q.; Dong, J.; Wang, C.; Liu, X.; Fang, G. An Enhanced Algorithm for Deinterleaving Mixed Radar Signals. *IEEE Trans. Aerosp. Electron. Syst.* **2021**, *57*, 3927–3940. [[CrossRef](#)]
21. Jiang, Q.; Ma, H. Estimation of Pulse Repetition Interval and Deinterleaving Based on the Square Sine Wave Interpolating Algorithm. *J. Electron. Inf. Technol.* **2007**, *29*, 350–354. [[CrossRef](#)]
22. Yu, Y.; Zhang, X. Jitter signal deinterleaving algorithm based on cumulative square sine wave interpolation. *Radar Countermeas.* **2013**, *33*, 12–16. [[CrossRef](#)]
23. Moore, J.B.; Krishnamurthy, V. Deinterleaving pulse trains using discrete-time stochastic dynamic-linear models. *IEEE Trans. Signal Process.* **1994**, *42*, 3092–3103. [[CrossRef](#)]
24. Conroy, T.; Moore, J.B. The limits of extended Kalman filtering for pulse train deinterleaving. *IEEE Trans. Signal Process.* **1998**, *46*, 3326–3332. [[CrossRef](#)]
25. Liu, J.; Meng, H.; Liu, Y.; Wang, X. Deinterleaving pulse trains in unconventional circumstances using multiple hypothesis tracking algorithm. *Signal Process.* **2010**, *90*, 2581–2593. [[CrossRef](#)]
26. Liu, Z.; Yu, P.S. Classification, Denoising, and Deinterleaving of Pulse Streams With Recurrent Neural Networks. *IEEE Trans. Aerosp. Electron. Syst.* **2019**, *55*, 1624–1639. [[CrossRef](#)]
27. Liu, Z.M. Online Pulse Deinterleaving With Finite Automata. *IEEE Trans. Aerosp. Electron. Syst.* **2020**, *56*, 1139–1147. [[CrossRef](#)]
28. Li, X.; Liu, Z.; Huang, Z. Deinterleaving of Pulse Streams With Denoising Autoencoders. *IEEE Trans. Aerosp. Electron. Syst.* **2020**, *56*, 4767–4778. [[CrossRef](#)]
29. Liu, Z.M. Pulse Deinterleaving for Multifunction Radars With Hierarchical Deep Neural Networks. *IEEE Trans. Aerosp. Electron. Syst.* **2021**, *57*, 3585–3599. [[CrossRef](#)]
30. Levanon, N.; Mozeson, E., Matched Filter. In *Radar Signals*; Wiley: Hoboken, NJ, USA, 2004; pp. 20–33. [[CrossRef](#)]
31. Zhuojun, X.; Hangwei, H.; Chengwei, X.; Wenting, Y.; Chunxu, L.; Chengzhi, Y.; Yantao, T. Stagger period estimation algorithm for multiple sets of radar pulses. *IET Radar Sonar Navig.* **2020**, *14*, 898–904. [[CrossRef](#)]

Disclaimer/Publisher’s Note: The statements, opinions and data contained in all publications are solely those of the individual author(s) and contributor(s) and not of MDPI and/or the editor(s). MDPI and/or the editor(s) disclaim responsibility for any injury to people or property resulting from any ideas, methods, instructions or products referred to in the content.